# Crystal structure of strontium hydrogen citrate monohydrate, $Sr(HC_6H_5O_7)(H_2O)$

James A. Kaduk [1,2,a)]
[1]Illinois Institute of Technology, 3101 S. Dearborn St., Chicago, Illinois 60616, USA
[2]North Central College, 30 N. Brainard St., Naperville, Illinois 60540, USA

(Received 26 January 2021; accepted 21 February 2021)

The crystal structure of strontium hydrogen citrate monohydrate has been solved using laboratory X-ray powder diffraction data, refined using both laboratory and synchrotron data, and optimized using density functional techniques. Strontium hydrogen citrate monohydrate crystallizes in space group *C*2/*c* (#15) with $a = 25.15601(17)$, $b = 10.90724(6)$, $c = 6.37341(4)$ Å, $\beta = 91.9846(6)°$, $V = 1747.704(12)$ Å$^3$, and $Z = 8$. The Sr coordination and the hydrogen bonding result in a layered structure. The $SrO_8$ coordination polyhedra share edges to form corrugated layers parallel to the *bc*-plane. Hydrogen bonds between the carboxylic acid groups and water molecules link the layers. Intermolecular hydroxyl–carboxyl hydrogen bonds also link the layers in a ring pattern with a graph set symbol *R2,2(12)*. After storage for 2 years, partial re-crystallization occurred, to an as-yet unknown compound with a triclinic unit cell. © *The Author(s), 2021. Published by Cambridge University Press on behalf of International Centre for Diffraction Data.*
[doi:10.1017/S0885715621000166]

Key words: citrate, strontium, Rietveld refinement, density functional theory

## I. INTRODUCTION

Citrate salts have a variety of industrial uses, including as polymer additives and chelating agents. Citrate is a common pharmaceutical counter-anion for cationic active pharmaceutical ingredients (APIs), and calcium citrate tetrahydrate is a widely used calcium supplement to reduce the effects of osteoporosis in women. Metal citrates are often used as reagents in the synthesis of ceramic oxides by the Pechini method. Citrate anions have a rich structural chemistry, reflecting their variable states of ionization, conformational flexibility, and variety of metal coordination modes.

A systematic study of the crystal structures of Group 1 (alkali metal) citrate salts has been reported in Rammohan and Kaduk (2018) and companion papers. The study was extended to mixed Group 1 citrate and to alkali/ammonium citrates in another series of papers. Recent work has extended the study to Group 2 (alkaline earth) citrates, including those of magnesium (Kaduk, 2020a), calcium (Kaduk, 2018, 2020b), and barium (Kaduk, 2021). This paper represents a further extension to strontium citrates.

A search of the Cambridge Structural Database (Groom *et al.*, 2016) for strontium citrates yielded only strontium citrate pentahydrate (Zacharias and Glusker, 1993; CSD Refcode LATRAZ). A similar search in the Powder Diffraction File (Gates-Rector and Blanton, 2019) yielded entry 02-067-4890, calculated from the LATRAZ structure.

## II. EXPERIMENTAL

Strontium hydrogen citrate monohydrate was prepared by adding 0.7366 g (5.0 mmol) $SrCO_3$ to a solution of 2.0771 g (10.0 mmol) $H_3C_6H_5O_7(H_2O)_1$ in 30 ml of water and heating slowly. ($SrCO_3$ does not react with citric acid solution at room temperature.) After slow fizzing, the solution became nearly clear after ~10 min. The solution was filtered and allowed to stand at ambient conditions. A small amount of white solid formed almost immediately as the solution cooled, so the mixture was filtered again. After 3 days at ambient conditions, a white solid formed, embedded in a yellow glass.

A laboratory X-ray powder pattern was measured (Cu$K\alpha$ radiation, 5–70° 2$\theta$, 0.0202144° steps, 1.0 s step$^{-1}$) on a Bruker D2 Phaser diffractometer equipped with a LynxEye position-sensitive detector. The pattern (Figure 1) was indexed on a *C*-centered monoclinic cell having $a = 25.1383$, $b = 10.8954$, $c = 6.3776$ Å, $\beta = 91.941°$, $V = 1745.8$ Å$^3$, and $Z = 8$ using N-TREOR (Altomare *et al.*, 2013). Analysis of the systematic absences using FOX (Favre-Nicolin and Černý, 2002) suggested the space group *C*2/*c*. The volume/asymmetric unit indicated that this was a 1:1 Sr:citrate salt, rather than the stoichiometric 1:2. The structure was solved using FOX using an Sr atom and a citrate anion as fragments, and a water molecule was added in the void suggested by Mercury (Macrae *et al.*, 2020).

Another pattern was measured (after storage at ambient conditions for 25 months; additional storage for 6 years did not result in further changes to the pattern) at 295 K at beamline 11-BM (Antao *et al.*, 2008; Lee *et al.*, 2008; Wang *et al.*, 2008) of the Advanced Photon Source at Argonne National Laboratory using a wavelength of 0.413353 Å from 0.5 to 50° 2$\theta$ with a step size of 0.001° and a counting time of 0.1 s step$^{-1}$. The white powder was packed into a 1.5-mm diameter Kapton capillary and rotated during the measurement at ~50 Hz. The synchrotron pattern (Figure 2) indicated that the sample had changed and was a mixture of phases.

The additional peaks were indexed on a primitive triclinic cell having $a = 8.9630$, $b = 11.7390$, $c = 13.7698$ Å, $\alpha =$

a)Author to whom correspondence should be addressed. Electronic mail: kaduk@polycrystallography.com

 © 2021 JCPDS-ICDD
https://doi.org/10.1017/S0885715621000166 Published online by Cambridge University Press

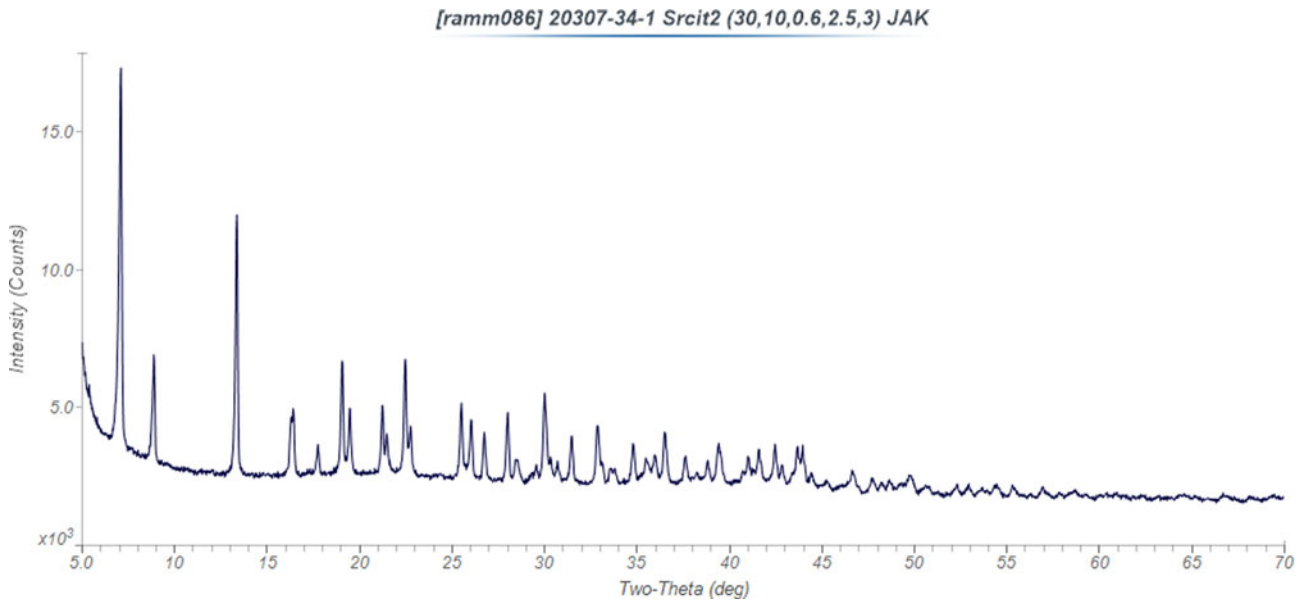



Figure 1. Laboratory (Cu$K\alpha$ radiation) of $Sr(HC_6H_5O_7)(H_2O)$, which crystallized from a synthesis with an Sr:citrate ratio = 1:2.

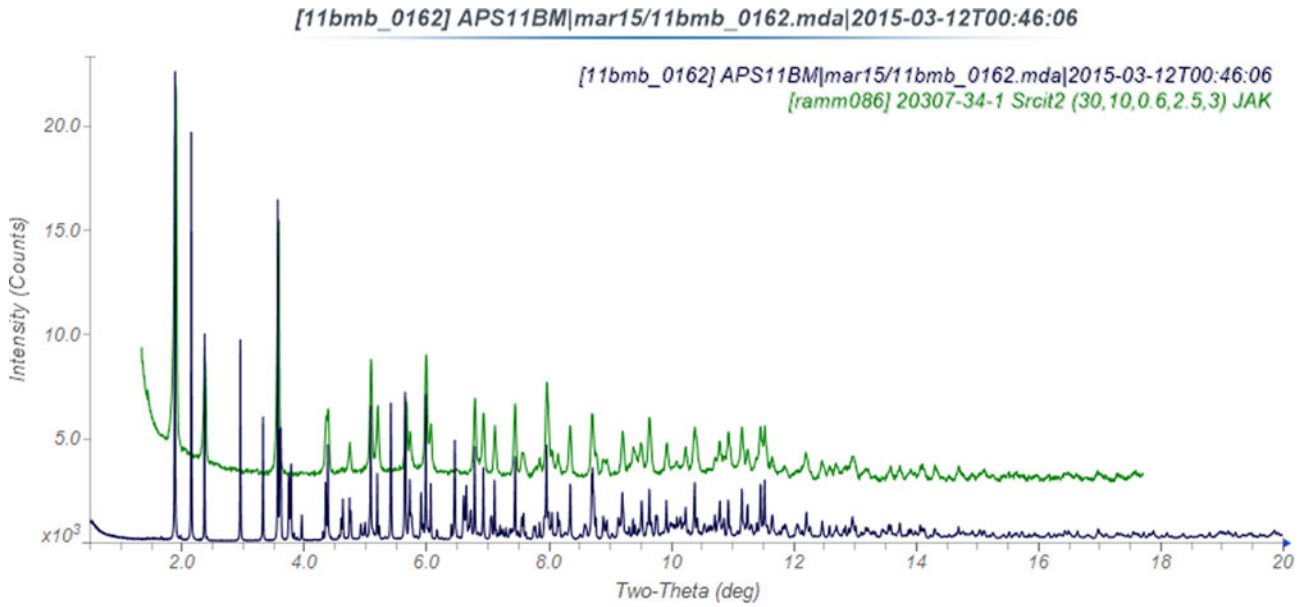



Figure 2. Comparison of the synchrotron (black) and laboratory (green) patterns of strontium hydrogen citrate monohydrate. The laboratory pattern was converted to the synchrotron wavelength of 0.413353 Å using Jade Pro (MDI, 2019).

97.984, $\beta = 101.871$, $\gamma = 106.433°$, and $V = 1329.59$ Å$^3$ using DICVOL14 (Louër and Boultif, 2014). The space group was assumed to be *P*-1. Using the 14.5 Å$^3$/non-H atom in strontium hydrogen citrate monohydrate and the 15.4 Å$^3$ in LATRAZ, this cell volume corresponds to 43-44 atoms in the asymmetric unit.

This second phase was included in a Rietveld refinement as a Le Bail phase. Its peaks account for a significant fraction of the pattern (Figure 3). The reflection list was extracted from the Crystallographic Information Framework (CIF) written by GSAS-II and converted into a *d/I* list using a spreadsheet. This peak list was used as input to Endeavour (Putz and Brandenburg, 2019). Initial attempts to solve the structure by Monte Carlo Simulated Annealing techniques using only Sr atoms as fragments yielded the lowest residuals with 4 Sr/cell. Four Sr/cell plus 6 citrates (13 atoms each) yields 82 atoms/cell, suggesting the presence of ~4–6 water molecules/cell. The original sample was obtained from a preparation with Sr:citrate = 1:2, so the presence of $Sr(Hcit)H_2O$ means that there was excess citrate present in the amorphous fraction. Over 2 years of storage, it is not unreasonable to expect additional crystallization, perhaps to yield a strontium citrate/citric acid co-crystal analogous to aqua(hydrogencitrato)(citric acid)calcium monohydrate, $[Ca(HC_6H_5O_7)(H_3C_6H_5O_7)(H_2O)](H_2O)$ (Kaduk, 2020b). Attempts to solve the structure using 4 Sr, 6 citrate, and 8 O/cell led to a best solution containing 2 Sr, 3 citrates, and 6 water molecules in the unit cell. Refinement of such a large structure in a mixture was not promising. A better solution for characterizing this compound will be to synthesize it in pure form.


https://doi.org/10.1017/S0885715621000166 Published online by Cambridge University Press

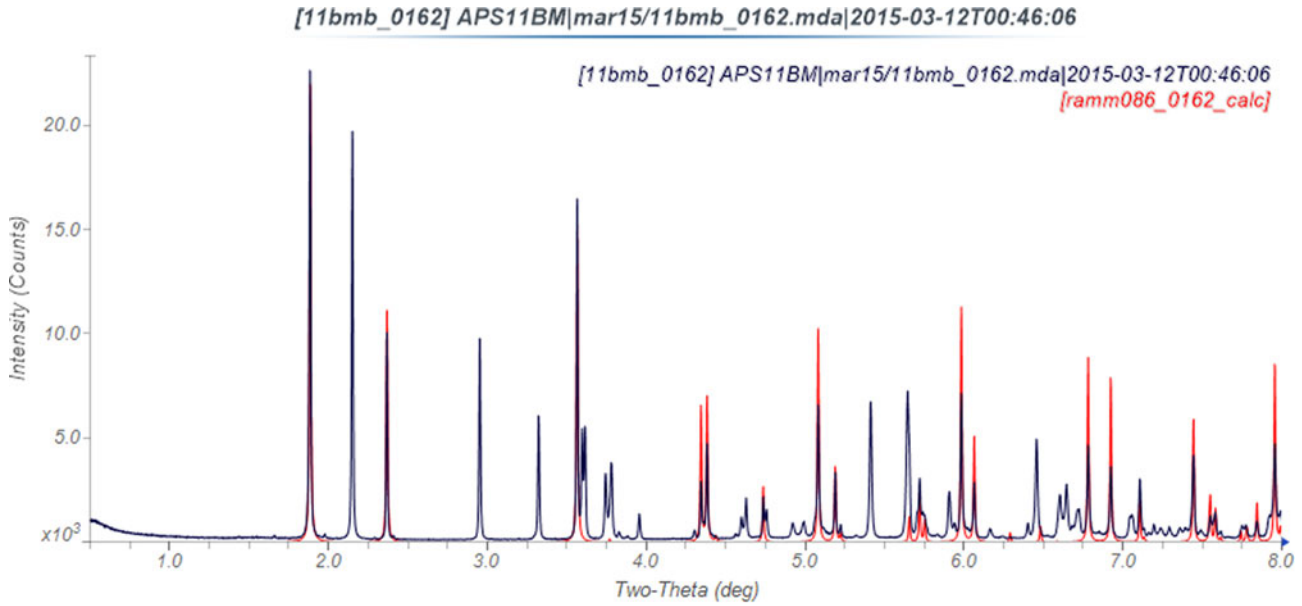



Figure 3. Comparison of the synchrotron pattern (black) to the pattern calculated for $Sr(HC_6H_5O_7)(H_2O)$, highlighting the peaks from the uncharacterized second phase with a triclinic unit cell.

The structure of strontium hydrogen citrate monohydrate was first refined with the laboratory data using GSAS-II (Toby and Von Dreele, 2013). The final refinement of 87 variables using 2968 observations and 36 restraints yielded the residuals $R_{wp} = 0.04696$ and GOF = 2.36. The structure was refined again with the synchrotron data using GSAS-II. The final refinement of 77 variables using 28 304 observations and 37 restraints yielded the residuals $R_{wp} = 0.11623$ and GOF = 2.69. A density functional geometry (DFT) optimization was carried out, along with a Mulliken population analysis, using CRYSTAL09 (Dovesi *et al.*, 2005). The basis sets for the H, C, and O atoms were those of Gatti *et al.* (1994), and the basis set for Sr was that of Piskunov *et al.* (2004). The calculation used 8 *k*-points and the B3LYP functional, and took ~4 days on a 2.4 GHz PC.

The structure contained $SrO_8$ coordination spheres, which joined into layers. The water molecule O21 was coordinated, and bridged two Sr. Several features of these structures suggested that the structure was incorrect, despite the low refinement residuals. The agreement of the two refined structures with the DFT-optimized structure was poor (Figure 4), and well outside the normal range for correct structures. The orientations of the central carboxylate groups C6/O15/O16 were significantly different in the two refined structures. Using the laboratory data, the position of the water molecule O21 refined to a location unreasonably close to the hydroxyl group O17. In both refinements, some of the displacement coefficients refined to unreasonable values.

These features suggested that the Monte Carlo Simulated Annealing structure solution had not found the global

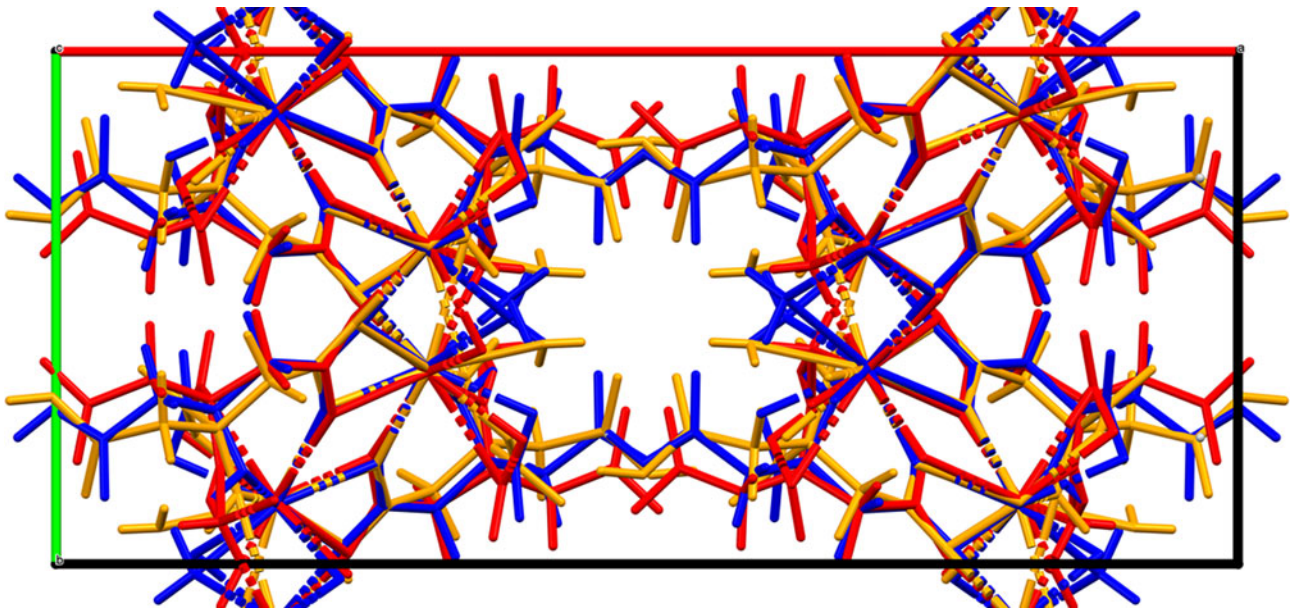


Figure 4. Comparison of the laboratory (red), synchrotron (orange), and DFT models of the initial incorrect structure of strontium hydrogen citrate monohydrate.


https://doi.org/10.1017/S0885715621000166 Published online by Cambridge University Press

minimum but had become trapped in a false minimum. Accordingly, two different strategies were used to search for the global minimum. FOX was used again, with a citrate, Sr, and two O atoms as fragments. The hope was that the dynamic occupancy correction feature would merge the two O atoms (water molecules) if they got too close to each other. All 150 trials yielded similar structures, which had some Sr–O distances which were far too short (<1.5 Å), and an unreasonable conformation of the citrate anions (two carboxyl groups too close to each other). Simultaneously, the simulated annealing feature of EXPO2014 (Altomare *et al.*, 2013) was applied, with a citrate, Sr, and one O as fragments. This attempt yields a much improved structure.

The new model of the structure of strontium hydrogen citrate monohydrate was first refined with the laboratory data using GSAS-II (Toby and Von Dreele, 2013). Only the 10.0–70.0° portion of the pattern was included in the refinement ($d_{min}$ = 1.343 Å), as the intensities of the lowest-angle peaks are affected by beam spillover, and are too low. All non-H bond distances and angles in the citrate anion were subjected to restraints, based on a Mercury/Mogul Geometry Check (Bruno *et al.*, 2004; Sykes *et al.*, 2011) of the cation and the anion. The Mogul average and standard deviation for each quantity were used as the restraint parameters. The Sr–O bonds were restrained to a value of 2.63(10) Å, based on the expected value for an 8-coordinate Sr by the bond valence method. The restraints contributed 12.3% to the final $\chi^2$. The hydrogen atoms were included in calculated positions, which were recalculated during the refinement using Materials Studio (Dassault, 2020). The $U_{iso}$ were grouped by chemical similarity; the $U_{iso}$ for the H atoms were fixed at 1.3× the $U_{iso}$ of the heavy atoms to which they are attached. The peak profiles were described using a uniaxial microstrain model, with 100 as the unique axis. The background was modeled using a 9-term shifted Chebyshev polynomial. A second-order spherical harmonic preferred orientation model was included; the texture index was 1.021(2).

The final refinement of 69 variables using 2968 observations and 37 restraints yielded the residuals $R_{wp}$ = 0.03037 and GOF = 1.52. The largest peak (2.02 Å from C4) and hole (2.39 Å from O13) in the difference Fourier map were 0.51 and −0.46(10) $e$Å$^{-3}$, respectively. The final fit (Figure 5) is excellent, and only minor errors are noted.

The structure of strontium hydrogen citrate monohydrate was refined again with the synchrotron data using GSAS-II (Toby and Von Dreele, 2013). Only the 1.3–30.0° portion of the pattern was included in the refinement ($d_{min}$ = 0.798 Å), and the same strategy was followed. The restraints contributed 1.0% to the final $\chi^2$. The peak profiles were described using the generalized microstrain model. The background was modeled using a 6-term shifted Chebyshev polynomial. A second-order spherical harmonic preferred orientation model was included; the texture index was 1.000(0).

The final refinement of 79 variables using 28 704 observations and 37 restraints yielded the residuals $R_{wp}$ = 0.09376 and GOF = 2.16. The largest peak (0.16 Å from Sr19) and hole (2.03 Å from O13) in the difference Fourier map were 0.43 and −0.42(11) $e$Å$^{-3}$, respectively. The largest errors in the fit (Figure 6) are in the shapes and positions of some of the peaks and may reflect changes in the specimen during exposure to the X-ray beam.

A DFT geometry optimization (fixed experimental unit cell) was carried out using VASP (Kresse and Furthmüller, 1996) through the MedeA graphical interface (Materials Design, 2016). The calculations were carried out on 16 2.4 GHz processors (each with 4 GB RAM) of a 64-processor HP Proliant DL580 Generation 7 Linux cluster at North Central College. The calculations used the GGA-PBE functional, a plane wave cutoff energy of 400.0 eV, and a $k$-point spacing of 0.5 Å$^{-1}$ leading to a 3 × 3 × 2 mesh. A single-point calculation was carried out, along with a Mulliken population analysis, using CRYSTAL14 (Dovesi *et al.*, 2014). The basis sets for the H, C, and O atoms were those of Gatti *et al.* (1994), and the basis set for Sr was that

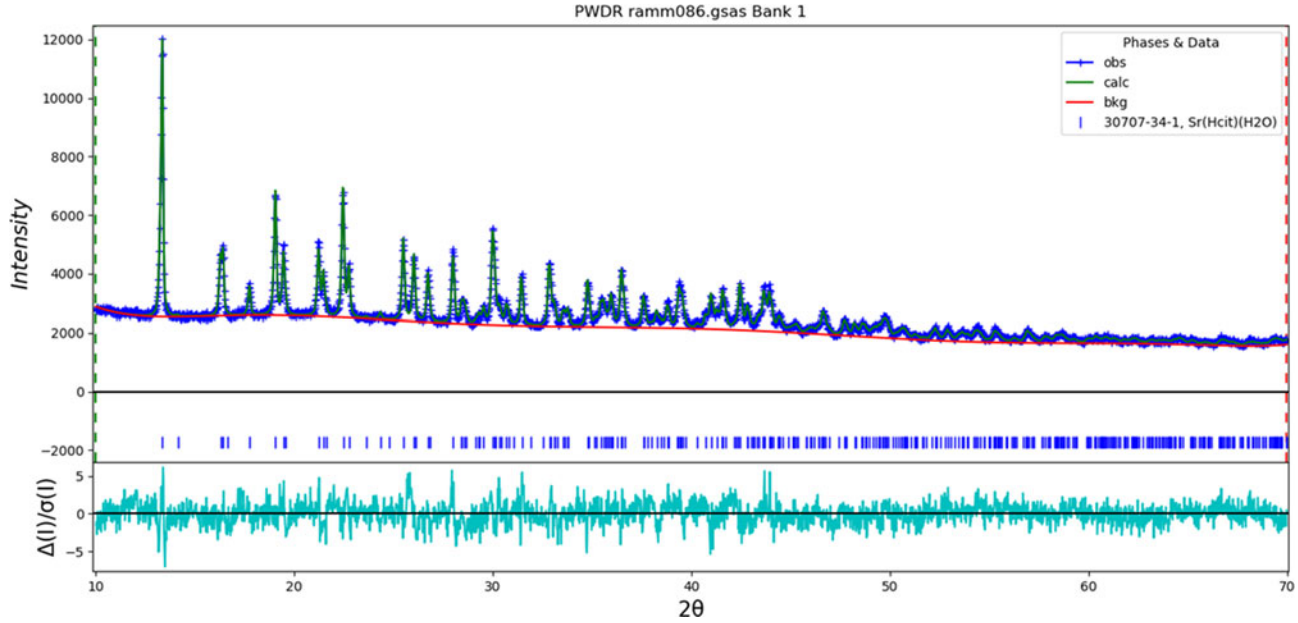



Figure 5. The Rietveld plot for the laboratory refinement of strontium hydrogen citrate monohydrate. The blue crosses represent the observed data points, and the green line is the calculated pattern. The cyan curve is the normalized error plot.


https://doi.org/10.1017/S0885715621000166 Published online by Cambridge University Press

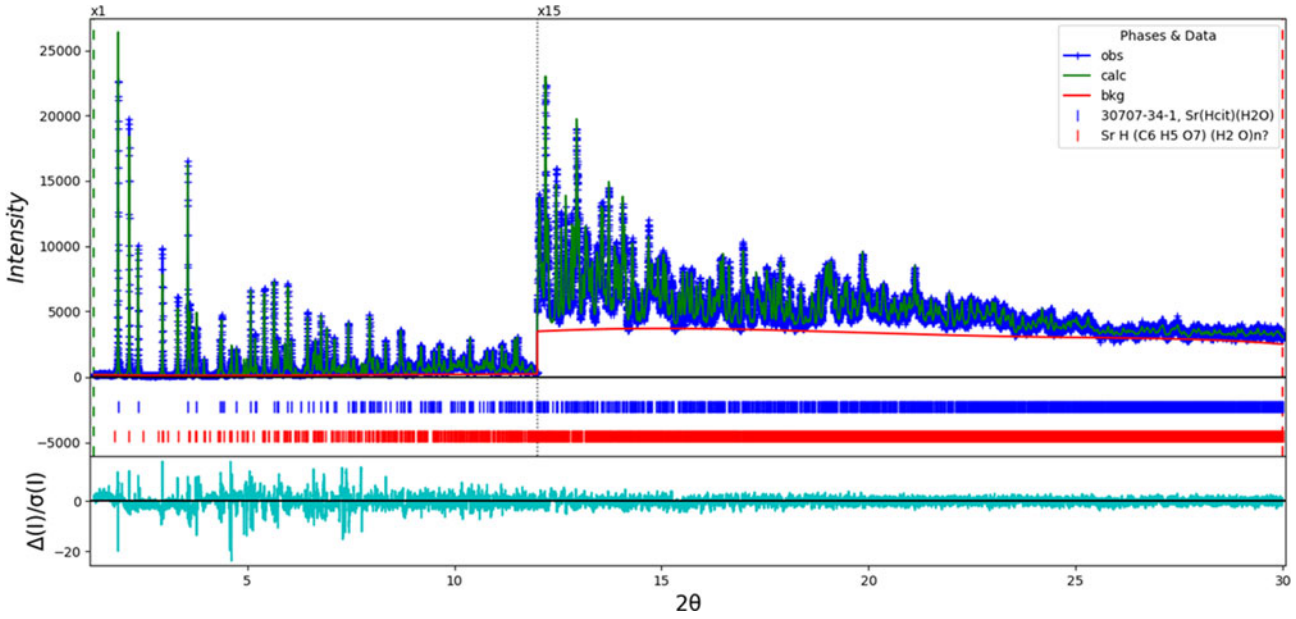



Figure 6. The Rietveld plot for the synchrotron refinement of strontium hydrogen citrate monohydrate. The blue crosses represent the observed data points, and the green line is the calculated pattern. The cyan curve is the normalized error plot. The vertical scale has been multiplied by a factor of 15× for $2\theta$ >12.0°.

of Laun *et al.* (2018). The calculations were run on 8 2.1 GHz Xeon cores (each with 6 GB RAM) of a 304-core Dell Linux cluster at IIT, used 8 *k*-points and the B3LYP functional.

## III. RESULTS AND DISCUSSION

The crystal structure of strontium hydrogen citrate monohydrate has been refined twice, once using laboratory (Cu$K\alpha$) data and once using synchrotron data from a sample containing a significant concentration of an unknown impurity. The structure has also been optimized using density functional techniques. The refined atom coordinates (both from the Rietveld refinements and the DFT optimization) are reported in the CIFs which have been deposited with ICDD. The atom numbering is shown in Figure 7, and the crystal structure is illustrated in Figure 8.

The root-mean-square (rms) Cartesian displacement between the laboratory and DFT structures is 0.076 Å, the rms displacement between the synchrotron and DFT structures is 0.087 Å, and the displacement between the laboratory and synchrotron structures is 0.066 Å. The structures are virtually identical, and the agreement is well within the normal range for correct structures (van de Streek and Neumann, 2014). The rest of this discussion will emphasize the DFT structure.

The citrate is ionized at the central and one of the terminal carboxyl groups, as is the typical pattern (Rammohan and

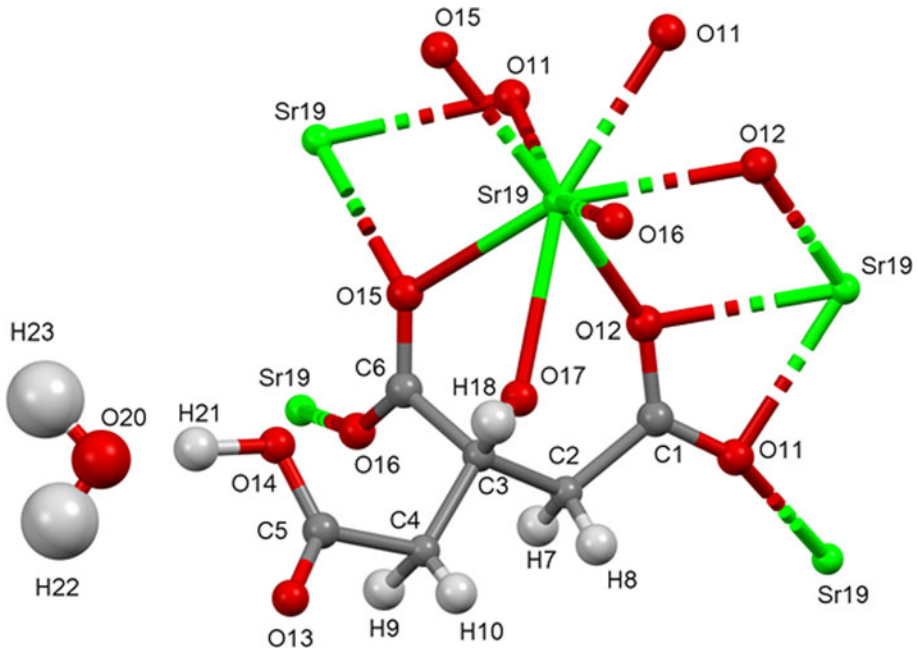



Figure 7. The atom numbering in strontium hydrogen citrate monohydrate. The atoms are represented by 50% probability spheroids.


https://doi.org/10.1017/S0885715621000166 Published online by Cambridge University Press

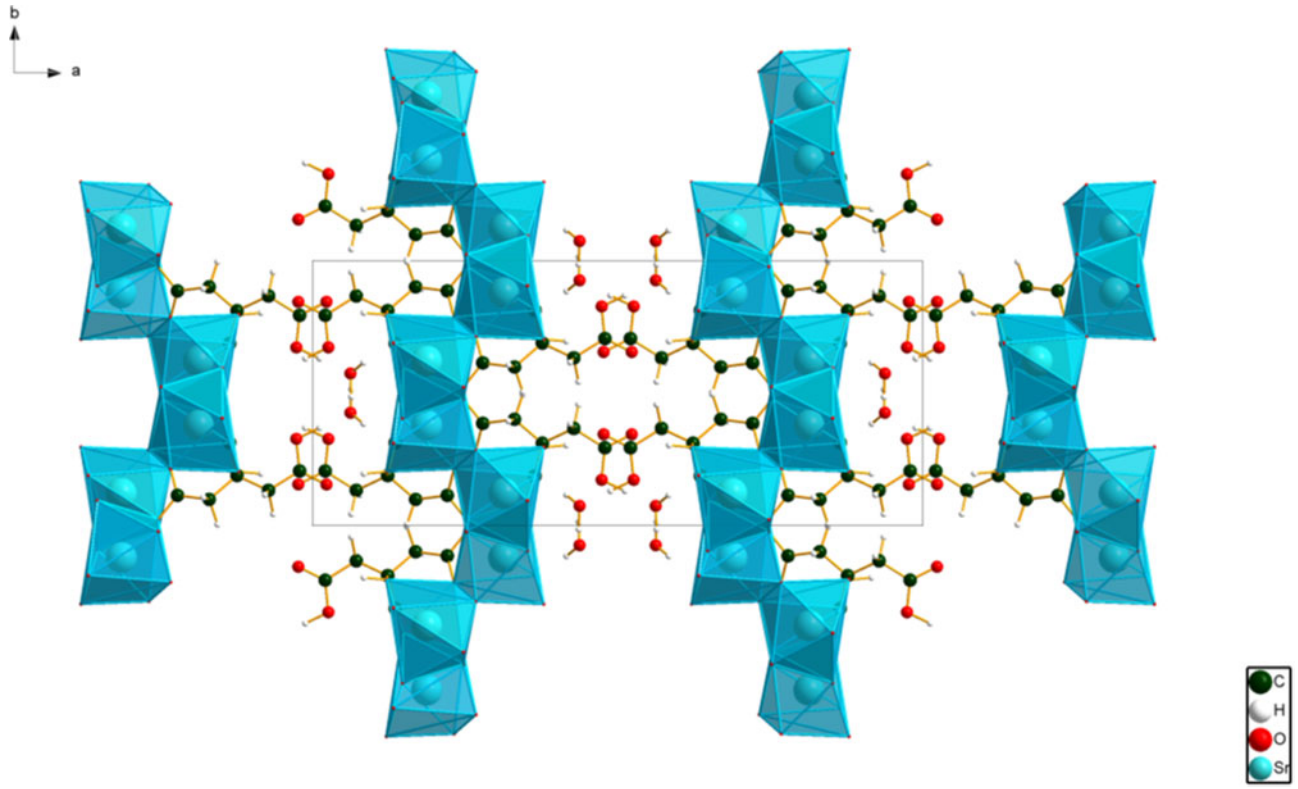



Figure 8. The crystal structure of strontium hydrogen citrate monohydrate, viewed down the *c*-axis.

Kaduk, 2018). The citrate triply chelates to an Sr19 through the central carboxylate O15, the terminal carboxylate O12, and the hydroxyl group O17. The carboxylate O11/O12 chelates to another Sr19. O11, O12, O15, and O16 each bridge two additional Sr19. The terminal carboxylic acid C5/O13/O14/H21 does not coordinate with the Sr. Unlike in the first wrong structure, the water molecule O20 does not coordinate to the Sr. The Sr is 8-coordinate (distorted square antiprism), and the bond valence sum is 2.15.

The Sr coordination and the hydrogen bonding result in a layered structure (Figure 8). The $SrO_8$ coordination polyhedra share edges to form corrugated layers parallel to the *bc*-plane. Hydrogen bonds between the carboxylic acid groups and water molecules link the layers. The hydrophobic methylene groups are adjacent to each other in the structure.

Almost all of the bond distances, bond angles, and torsion angles fall within the normal ranges indicated by a Mercury/Mogul Geometry Check (Macrae *et al.*, 2020). The O17–C3–C6 angle of 111.1° (average = 107.5(11)°, *Z*-score = 3.3) is flagged as unusual. The standard uncertainty on the average is relatively small and the population of similar angles is small; both of these inflate the *Z*-score. The O13–C5–C4–C3 and O14–C5–C4–C3 torsion angles are flagged as unusual. These lie on the tails of very broad distributions, and the terminal carboxyl groups can have nearly any torsion angle in citrates (Rammohan and Kaduk, 2018). The citrate anion is in the *trans,trans* conformation, which is one of the two low-energy conformations of citrate anions, and is typical for salts containing larger cations (Rammohan and Kaduk, 2018). The central portion of the molecule is in the usual planar arrangement; the O17–C3–C6–O15 torsion angle is 8.0°.

Analysis of the contributions to the total crystal energy using the Forcite module of Materials Studio (Dassault, 2020) suggests that angle distortion terms dominate the intramolecular deformation energy, but that bond and torsion terms also are significant. The intermolecular energy is dominated by electrostatic attractions, which in this force-field-based analysis include cation coordination and hydrogen bonds. The hydrogen bonds are better analyzed using the results of the DFT calculation.

The carboxylic acid O14–H21 acts as the donor in a strong hydrogen bond to the water molecule O20 (Table I). The water molecule acts as a donor in two hydrogen bonds, one to the ionized carboxylate O16 and the other to the unionized carboxylic acid O14. The hydroxyl group O17–H18 is the donor in an intermolecular hydrogen bond to the carbonyl group O13. These hydrogen bonds link the layers in a ring

TABLE I. Hydrogen bonds (CRYSTAL09) in strontium hydrogen citrate monohydrate.

| H-Bond | D-H (Å) | H···A (Å) | D···A (Å) | D-H···A (°) | Mulliken Overlap (*e*) | *E* (kcal mol$^{-1}$) |
|---|---|---|---|---|---|---|
| O14–H21···O20 | 1.066 | 1.435 | 2.501 | 177.6 | 0.072 | 14.7 |
| O20–H22···O16 | 1.001 | 1.678 | 2.648 | 161.8 | 0.042 | 11.2 |
| O20–H23···O14 | 0.981 | 2.002 | 2.848 | 143.2 | 0.029 | 9.3 |
| O17–H18···O13 | 0.992 | 1.772 | 2.751 | 166.5 | 0.057 | 13.0 |


https://doi.org/10.1017/S0885715621000166 Published online by Cambridge University Press

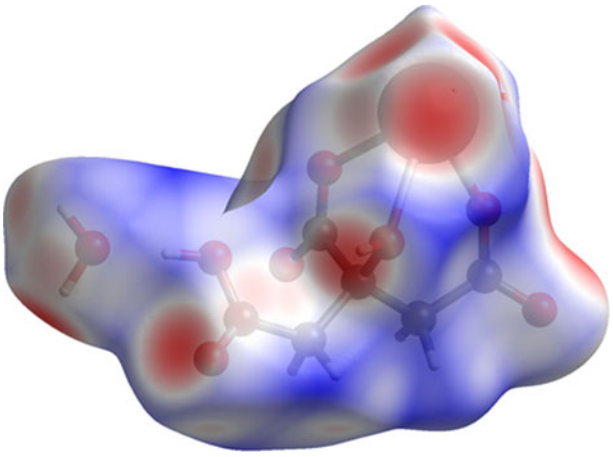


Figure 9. The Hirshfeld surface of strontium hydrogen citrate monohydrate. Intermolecular contacts longer than the sums of the van der Waals radii are colored blue, and contacts shorter than the sums of the radii are colored red. Contacts equal to the sums of radii are white.

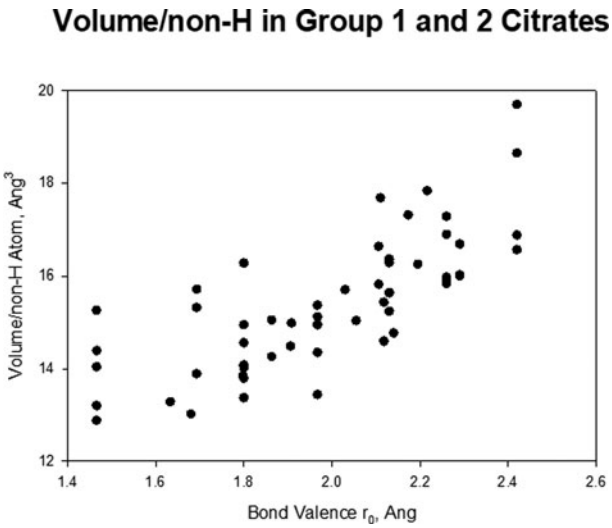



Figure 10. Correlation between the cation size (measured by the bond valence $r_0$) and the volume/non-H atom in Group 1 and Group 2 citrates. The $r_0$ for $Sr^{2+}$–$O^{2-}$ = 2.118 Å.

pattern with a graph set symbol *R2,2(12)* (Etter, 1990; Bernstein *et al.*, 1995; Shields *et al.*, 2000).

The volume enclosed by the Hirshfeld surface (Figure 9; Hirshfeld, 1977; Turner *et al.*, 2017) is 206.56 Å$^3$, 94.55% of 1/8 the unit cell volume. The packing density is thus unusually high. All of the significant-close contacts (red in Figure 9) involve the hydrogen bonds and the Sr coordination. The volume/non-hydrogen atom is only 14.5 Å$^3$, smaller than the usual rule of thumb (17–18 Å$^3$/non-H atom), but falls within the trend for Group 1 and Group 2 citrates (Figure 10).

The Bravais–Friedel–Donnay–Harker (Bravais, 1866; Friedel, 1907; Donnay and Harker, 1937) method suggests that we might expect elongated morphology for strontium hydrogen citrate monohydrate, with ⟨001⟩ as the long axes, or platy morphology with {200} as the major faces. An second-order spherical harmonic model for the preferred orientation was incorporated into the laboratory refinement. The texture index was 1.021(2), indicating that the preferred orientation was slight in this rotated flat-plate specimen. A second-order model was included in the synchrotron refinement. The texture index was only 1.000(0), indicating that the preferred orientation was not present in that rotated capillary specimen.

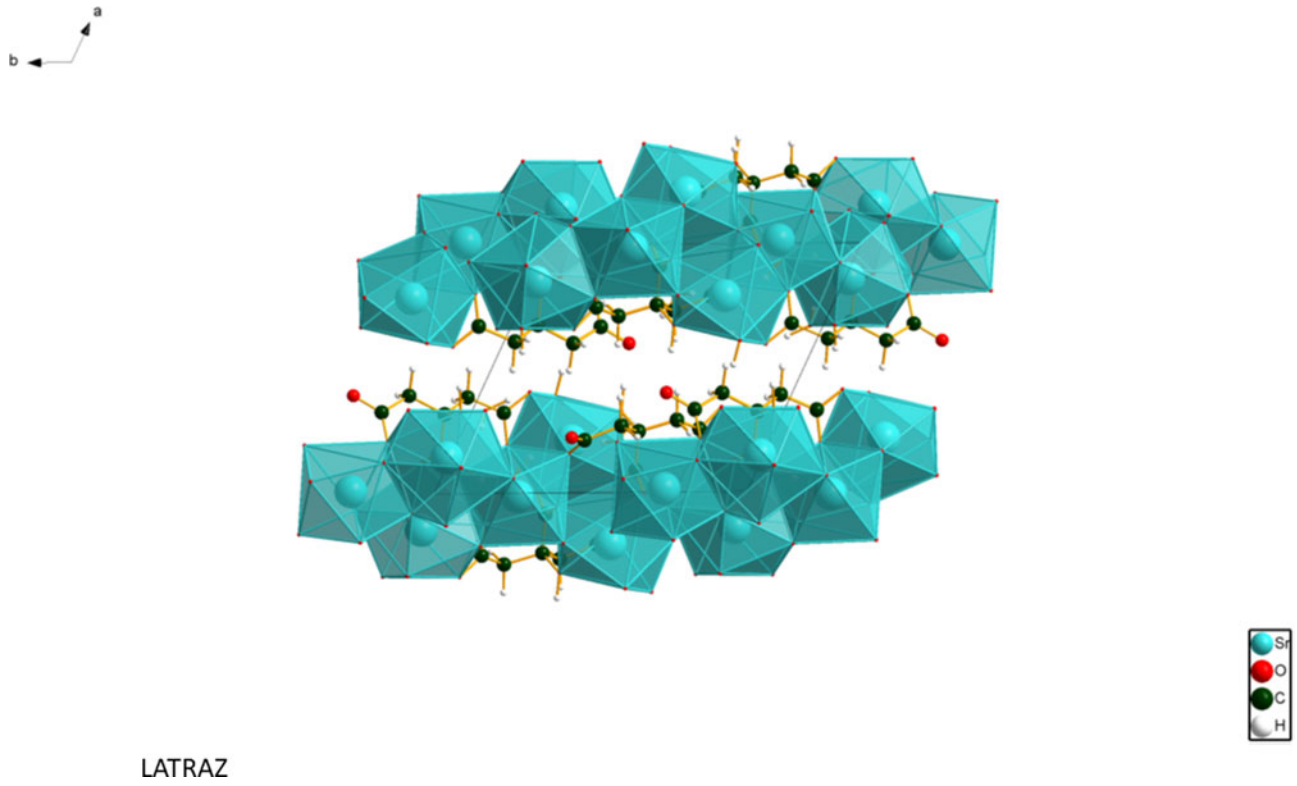



Figure 11. The crystal structure of tristrontium dicitrate pentahydrate (LATRAZ), viewed down the *c*-axis.


https://doi.org/10.1017/S0885715621000166 Published online by Cambridge University Press

TABLE II. Hydrogen bonds (CRYSTAL09) in tristrontium dicitrate pentahydrate (LATRAZ).

| H-Bond | D-H (Å) | H···A (Å) | D···A (Å) | D-H···A (°) | Mulliken Overlap (*e*) | *E* (kcal mol$^{-1}$) |
|---|---|---|---|---|---|---|
| O8–H54···O7 | 0.975 | 1.893 | 2.827 | 159.5 | 0.053 | 12.6 |
| O8–H53···O6 | 0.975 | 1.836 | 2.683 | 143.7 | 0.048 | 12.0 |
| O7–H52···O11 | 0.975 | 1.963 | 2.845 | 149.3 | 0.041 | 11.1 |
| O7–H51···O10 | 0.992 | 1.764 | 2.756 | 178.1 | 0.067 | 14.1 |
| O6–H50···O9 | 0.970 | 2.289 | 3.011 | 130.3 | 0.016 | 6.9 |
| O6–H50···O14 | 0.970 | 2.289 | 3.077 | 137.7 | 0.016 | 6.9 |
| O6–H49···O27 | 0.971 | 1.805 | 2.768 | 171.1 | 0.052 | 12.5 |
| O5–H48···O11 | 0.986 | 1.854 | 2.827 | 168.7 | 0.062 | 13.6 |
| O5–H47···O22 | 0.998 | 1.764 | 2.731 | 162.2 | 0.071 | 14.6 |
| O4–H46···O14 | 0.983 | 1.869 | 2.788 | 154.5 | 0.056 | 12.9 |
| O4–H45···O11 | 0.991 | 1.801 | 2.742 | 157.3 | 0.061 | 13.5 |
| O28–H36···O25 | 0.979 | 1.648 | 2.617 | 169.8 | 0.072 | 14.7 |
| O15–H35···O22 | 0.991 | 1.730 | 2.721 | 162.2 | 0.070 | 14.5 |
| C17–H37···O27 | 1.096 | 2.311 | 3.337 | 155.1 | 0.028 | |
| C30–H42···O25 | 1.093 | 2.390 | 3.179 | 127.8 | 0.015 | |

In the structure of LATRAZ, the three independent Sr are 8-, 8-, and 9-coordinate. The coordination polyhedra share edges to form layers parallel to the *bc*-plane (Figure 11). Only van der Waals interactions seem to occur between the layers. The citrates are also in the *trans,trans* conformation. The high number of water molecules means that the hydrogen bonding (Table II) is very different than in $Sr(HC_6H_5O_7)(H_2O)$. Larger numbers of strontium citrate structures will be required before more detailed conclusions about trends can be made.

## IV. DEPOSITED DATA

The Crystallographic Information Framework (CIF) files containing the results of the Rietveld refinements (including the raw data) and the DFT geometry optimization were deposited with the ICDD. The data can be requested at info@icdd.com.

## ACKNOWLEDGEMENTS

The use of the Advanced Photon Source at Argonne National Laboratory was supported by the U.S. Department of Energy, Office of Science, Office of Basic Energy Sciences, under Contract No. DE-AC02-06CH11357. I thank Lynn Ribaud and Saul Lapidus for their assistance in the data collection. I thank an anonymous reviewer for the suggestion that the first structure was a false minimum and that the structure solution should be explored further. I thank Andrey Roachev for the use of computing resources at IIT.

## CONFLICTS OF INTEREST

The author has no conflicts of interest to declare.

Altomare, A., Cuocci, C., Giacovazzo, C., Moliterni, A., Rizzi, R., Corriero, N., and Falcicchio, A. (**2013**). "EXPO2013: a kit of tools for phasing crystal structures from powder data," J. Appl. Crystallogr. **46**, 1231–1235.

Antao, S. M., Hassan, I., Wang, J., Lee, P. L., and Toby, B. H. (**2008**). "State-of-the-art high-resolution powder X-ray diffraction (HRPXRD) illustrated with Rietveld refinement of quartz, sodalite, tremolite, and meionite," Can. Mineral. **46**, 1501–1509.

Bernstein, J., Davis, R. E., Shimoni, L., and Chang, N. L. (**1995**). "Patterns in hydrogen bonding: functionality and graph set analysis in crystals," Angew. Chem. Int. Ed. Engl. **34**, 1555–1573.

Bravais, A. (**1866**). *Etudes Cristallographiques* (Gauthier Villars, Paris).

Bruno, I. J., Cole, J. C., Kessler, M., Luo, J., Motherwell, W. D. S., Purkis, L. H., Smith, B. R., Taylor, R., Cooper, R. I., Harris, S. E., and Orpen, A. G. (**2004**). "Retrieval of crystallographically-derived molecular geometry information," J. Chem. Inf. Sci. **44**, 2133–2144.

Dassault Systèmes (**2020**). *Materials Studio 2020* (BIOVIA, San Diego, CA).

Donnay, J. D. H. and Harker, D. (**1937**). "A new law of crystal morphology extending the law of Bravais," Am. Mineral. **22**, 446–447.

Dovesi, R., Orlando, R., Civalleri, B., Roetti, C., Saunders, V. R., and Zicovich-Wilson, C. M. (**2005**). "CRYSTAL: a computational tool for the *ab initio* study of the electronic properties of crystals," Z. Kristallogr. **220**, 571–573.

Dovesi, R., Orlando, R., Erba, A., Zicovich-Wilson, C. M., Civalleri, B., Casassa, S., Maschio, L., Ferrabone, M., De Le Pierre, M., D'Arco, P., Noel, Y., Causa, M., Rerat, M., and Kirtman, B. (**2014**). "CRYSTAL14: a program for the *ab initio* investigation of crystalline solids," Int. J. Quantum Chem. **114**, 1287–1317.

Etter, M. C. (**1990**). "Encoding and decoding hydrogen-bond patterns of organic compounds," Acc. Chem. Res. **23**, 120–126.

Favre-Nicolin, V. and Černý, R. (**2002**). "FOX, Free objects for crystallography: a modular approach to ab initio structure determination from powder diffraction," J. Appl. Crystallogr. **35**, 734–743.

Friedel, G. (**1907**). "Etudes sur la loi de Bravais," Bull. Soc. Fr. Mineral. **30**, 326–455.

Gates-Rector, S. and Blanton, T. (**2019**). "The Powder Diffraction File: a quality materials characterization database," Powd. Diffr. **39**, 352–360.

Gatti, C., Saunders, V. R., and Roetti, C. (**1994**). "Crystal-field effects on the topological properties of the electron-density in molecular crystals – the case of urea," J. Chem. Phys. **101**, 10686–10696.

Groom, C. R., Bruno, I. J., Lightfoot, M. P., and Ward, S. C. (**2016**). "The Cambridge Structural Database," Acta Crystallogr. B: Struct. Sci., Cryst. Eng. Mater. **72**, 171–179.

Hirshfeld, F. L. (**1977**). "Bonded-atom fragments for describing molecular charge densities," Theor. Chem. Acta **44**, 129–138.

Kaduk, J. A. (**2018**). "Crystal structures of tricalcium citrates," Powd. Diffr. **33**, 237–243.

Kaduk, J. A. (**2020a**). "Crystal structures of two magnesium citrates from powder diffraction data," Acta Cryst. E **76**, 1611–1616.

Kaduk, J. A. (**2020b**). "Crystal structure of aqua(hydrogencitrato)(citric acid) calcium monohydrate, $[Ca(HC_6H_5O_7)(H_3C_6H_5O_7)(H_2O)](H_2O)$ from synchrotron X-ray powder data, and DFT-optimized crystal structure of existing calcium hydrogen citrate trihydrate, $[Ca(HC_6H_5O_7)(H_2O)_3]$," Acta Cryst. E **76**, 1689–1693.

Kaduk, J. A. (**2021**). "Tribarium dicitrate pentahydrate, $[Ba_3(C_6H_5O_7)_2(H_2O)_4](H_2O)$," Acta Cryst. E **77**, 251–254.

Kresse, G. and Furthmüller, J. (**1996**). "Efficiency of ab-initio total energy calculations for metals and semiconductors using a plane-wave basis set," Comput. Mater. Sci. **6**, 15–50.



https://doi.org/10.1017/S0885715621000166 Published online by Cambridge University Press

Laun, J., Oliveira, D. V., and Bredow, T. (**2018**). "Consistent Gaussian basis sets of double- and triple-zeta valence with polarization quality of the fifth period for solid-state calculations," J. Comput. Chem. **39**, 1285–1290. doi:10.1002/jcc.25195

Lee, P. L., Shu, D., Ramanathan, M., Preissner, C., Wang, J., Beno, M. A., Von Dreele, R. B., Ribaud, L., Kurtz, C., Antao, S. M., Jiao, X., and Toby, B. H. (**2008**). "A twelve-analyzer detector system for high-resolution powder diffraction," J. Synchrotron Radiat. **15**, 427–432.

Louër, D. and Boultif, A. (**2014**). "Some further considerations in powder diffraction pattern indexing with the dichotomy method," Powd. Diffr. **29**, S7–S12.

Macrae, C. F., Sovago, I., Cottrell, S. J., Galek, P. T. A., McCabe, P., Pidcock, E., Platings, M., Shields, G. P., Stevens, J. S., Towler, M., and Wood, P. A. (**2020**). "*Mercury 4.0:* from visualization to design and prediction," J. Appl. Crystallogr. **53**, 226–235.

Materials Design (**2016**). *MedeA 2.20.4* (Materials Design Inc., Angel Fire, NM).

MDI (**2019**). *JADE Pro Version 7.8 (Computer Software)* (Materials Data, Livermore, CA, USA).

Putz, H. and Brandenburg, K. (**2019**). Endeavour - Structure Solution from Powder Data Version 1.8b. Crystal Impact, Kreuzherrenstr. 102, Bonn, Germany. Available at: http://www.crystalimpact.com/endeavour.

Rammohan, A. and Kaduk, J. A. (**2018**). "Crystal structures of alkali metal (group 1) citrate salts," *Acta Crystallogr. B: Cryst. Eng. Mater*. **74**, 239–252. doi:10.1107/S2052520618002330.

Shields, G. P., Raithby, P. R., Allen, F. H., and Motherwell, W. S. (**2000**). "The assignment and validation of metal oxidation states in the Cambridge Structural Database," Acta Crystallogr. B: Struct. Sci. **56**, 455–465.

Sykes, R. A., McCabe, P., Allen, F. H., Battle, G. M., Bruno, I. J., and Wood, P. A. (**2011**). "New software for statistical analysis of Cambridge Structural Database data," J. Appl. Crystallogr. **44**, 882–886.

Toby, B. H. and Von Dreele, R. B. (**2013**). "GSAS II: the genesis of a modern open source all purpose crystallography software package," J. Appl. Crystallogr. **46**, 544–549.

Turner, M. J., McKinnon, J. J., Wolff, S. K., Grimwood, D. J., Spackman, P. R., Jayatilaka, D., and Spackman, M. A. (**2017**). *CrystalExplorer17* (University of Western Australia). Available at: http://hirshfeldsurface.net.

van de Streek, J. and Neumann, M. A. (**2014**). "Validation of molecular crystal structures from powder diffraction data with dispersion-corrected density functional theory (DFT-D)," Acta Crystallogr. B: Struct. Sci., Cryst. Eng. Mater. **70**, 1020–1032.

Wang, J., Toby, B. H., Lee, P. L., Ribaud, L., Antao, S. M., Kurtz, C., Ramanathan, M., Von Dreele, R. B., and Beno, M. A. (**2008**). "A dedicated powder diffraction beamline at the Advanced Photon Source: commissioning and early operational results," Rev. Sci. Instrum. **79**, 085105.

Zacharias, D. E. and Glusker, J. P. (**1993**). "Structure of strontium citrate pentahydrate," Acta Crystallogr. C: Cryst. Struct. Commun. **49**, 1732–1735. CSD Refcode LATRAZ.



https://doi.org/10.1017/S0885715621000166 Published online by Cambridge University Press